

Cosmology Interfaces of the TFPT Closed Branch

Seam Transfer, Axion Sector, Reheating, and CMB Targets

Stefan Hamann

Alessandro Rizzo

Paper 6 of the TFPT 4.5 series – April 27, 2026

Abstract

This paper isolates the downstream cosmology interface of TFPT. Cosmology is not used as a primitive selector of the theory. It is read from the closed branch through seam transfer, determinant-line phase, scalaron sector, axion interface, reheating input, leptogenesis input, neutrino sector, CMB spectra, and conjectural sky-map realization targets.

Scope box: inputs, contribution, non-claims, audit surface

Inputs from previous papers. Papers 1–5 supply the closed branch \mathfrak{T}_* , the carrier packet, the precision branch, the admissible QFT sector, and the boundary-normalized metrology.

New theorem contribution. Downstream cosmology interfaces:

$$\Lambda_{\text{IR}} = M_{\text{Pl}}^4 \left[-\log \det_{\text{adm}}(1 - U_{\Sigma}) \right], \quad S_{\Sigma} = \log \mu_{\Sigma}(\alpha_*), \quad N_{\text{DW}} = 1,$$

with axion, reheating, leptogenesis, and CMB targets stated at their proper status levels.

Not claimed here. No carrier proofs, no full α derivation, no QFT closure proof, and no Standard-Model packet proof.

Falsification or audit surface. The paper fails if CMB Stage 2 is sold as a theorem, if a good CMB world is conflated with this observed sky realization, or if cosmology is allowed to tune the primitive branch.

Editorial guardrail

CMB and E8 must never be written as hard theorem claims in this paper. Stage 1 is spectra. Stage 2 is sky realization as a conjectural or programmatic target.

Claim contract

Claim. Closed branch exports cosmology interface data: seam transfer, axion interface, reheating/leptogenesis inputs, and CMB Stage 1/2 targets.

Inputs. Fixed \mathfrak{T}_* , metrology layer, determinant-line phase, scalaron and neutrino sectors.

First assumptions. Infrared continuation and nonequilibrium solver are separate comparison-layer inputs.

Proof status. Downstream interface; Stage 2 sky realization is programmatic/conjectural.

Kill condition. Cosmology tunes the primitive branch or Stage 2 is presented as theorem-level sky reconstruction.

Contents

1 Cosmology as Downstream Interface

2

2	Seam Transfer and Infrared Determinant	2
3	Axion Interface	2
4	Reheating, Leptogenesis, and Neutrino Inputs	2
5	CMB Stage 1: Spectra	3
6	CMB Stage 2: Sky Realization	3
7	Downstream Obligations Moved to the Companion	3
8	Main Technical Development	4
9	FRW reduction, seam transfer, and the scalaron branch	4
9.1	Falsification matrix	8
9.2	Proof-obligation ledger	9
9.3	Infrared continuations of the seam transfer	10
10	FRW reduction and cosmology interface proofs	12
10.1	Axion interface	13
11	Source Extraction Map	13
12	Not Used Here	13

1 Cosmology as Downstream Interface

The closed branch is fixed before cosmology enters:

$$\mathfrak{T}_* \Rightarrow (U_\Sigma, \det_{\text{adm}}, \text{scalaron branch}, \text{neutrino sector}) \Rightarrow \text{cosmology interfaces.}$$

This section should make the nonprimitive status of cosmology explicit.

2 Seam Transfer and Infrared Determinant

The seam-transfer expression is

$$\Lambda_{\text{IR}} = M_{\text{Pl}}^4 \left[-\log \det_{\text{adm}}(1 - U_\Sigma) \right].$$

The text should state which part is theorem-level interface data and which part is an empirical comparison convention.

3 Axion Interface

The axion sector is recorded as

$$S_\Sigma = \log \mu_\Sigma(\alpha_*), \quad N_{\text{DW}} = 1, \quad \theta_i = \pi(1 - \varphi_\Sigma(\alpha_*)).$$

The axion interface belongs here because it depends on seam transfer and determinant-line phase, not on the primitive carrier proof.

4 Reheating, Leptogenesis, and Neutrino Inputs

Reheating and leptogenesis are stated as downstream inputs supplied by the closed branch. The paper should keep them status-coded and avoid turning the module into a hidden fit engine for later CMB targets.

5 CMB Stage 1: Spectra

Stage 1 is the spectral target: transfer functions, angular spectra, and comparison rows. This stage may define falsification targets and benchmark rows, but it does not claim a unique sky-map realization.

6 CMB Stage 2: Sky Realization

Stage 2 is a conjectural realization target. The source draft's distinction should remain explicit: a good CMB world is not automatically this CMB world. The map-realization layer therefore belongs in a programmatic or conditional section, not in the theorem stack.

7 Downstream Obligations Moved to the Companion

Module	Status in this paper
Stationary horizons and compact objects	Listed only as downstream programmatic obligations; technical material is in the Companion.
Code subspace, pointer dynamics, and record algebra	Not part of the cosmology-interface proof surface.
Transient event channels	Falsification and prediction semantics belong to the Companion.
Pole masses, Higgs readout, and full flavor output	Inputs from earlier readout papers or Companion ledgers, not cosmology claims.
Extended comparison ledgers	Companion-only material.

8 Main Technical Development

This section contains the main technical development assigned to this paper by the TFPT 4.5 clean split. Cross-paper background is referenced through dependency and scope boxes; extended backend material is kept in the Technical Companion.

9 FRW reduction, seam transfer, and the scalaron branch

The trace-class seam transfer belongs to the main reconstruction surface. The cosmological constant and the reduced scalaron / determinant-line dynamics are therefore fixed directly on the closed branch. Axion, reheating, and leptogenesis quantities are read through explicit interface formulas built from the same theorem-level objects U_Σ , a_Σ , and the positive scalaron sector \mathcal{H}_{sc} .

Theorem 9.1 (Trace-class seam transfer). *On the closed branch the seam transfer operator*

$$U_\Sigma := P_{\text{adm}} e^{-\ell_\Sigma |B_\Sigma|} P_{\text{adm}}$$

is positive and trace class. Hence

$$0 < \rho(U_\Sigma) < 1, \quad 0 < U_\Sigma < P_{\text{adm}}.$$

so the Fredholm determinant

$$-\log \det_{\text{adm}}(1 - U_\Sigma)$$

converges absolutely and defines a positive quantity.

Proposition 9.2 (Seam damping readout from electromagnetic closure). Let α_* be the unique electromagnetic fixed point of [TFPT cross-reference: thm:alpha-canonical]. Define the closed seam damping by

$$S_\Sigma := -\log \rho(U_\Sigma).$$

Then

$$S_\Sigma = \log \mu_\Sigma(\alpha_*) = \log(\varphi_\Sigma(\alpha_*)^{-1}) = \frac{\alpha_*^2(\alpha_* - 2c_3^3)}{8c_3^6 b_1}.$$

Proof. At the electromagnetic fixed point, [TFPT cross-reference: eq:carrier-cfe] is equivalent to

$$\log \mu_\Sigma(\alpha_*) = \frac{\alpha_*^2(\alpha_* - 2c_3^3)}{8c_3^6 b_1}.$$

The seam transfer operator

$$U_\Sigma = P_{\text{adm}} e^{-\ell_\Sigma |B_\Sigma|} P_{\text{adm}}$$

uses the same admissible determinant sector as the electromagnetic closure. Its spectral radius therefore defines the same exponential damping scale, so

$$S_\Sigma = \log \mu_\Sigma(\alpha_*) = \log(\varphi_\Sigma(\alpha_*)^{-1}).$$

□

Theorem 9.3 (Infrared cosmological constant from seam transfer).

$$U_\Sigma := P_{\text{adm}} e^{-\ell_\Sigma |B_\Sigma|} P_{\text{adm}}, \quad S_\Sigma := -\log \rho(U_\Sigma) = \log \mu_\Sigma(\alpha_*),$$

Then

$$\Lambda_{\text{IR}} = M_{\text{Pl}}^4 \left[-\log \det_{\text{adm}}(1 - U_\Sigma) \right]$$

is well defined and positive on the closed branch, and

$$0 < U_\Sigma \leq e^{-S_\Sigma} P_{\text{adm}} < P_{\text{adm}}.$$

Proof. Theorem 9.1 gives trace-class positivity of U_Σ , while Proposition 9.2 fixes the intrinsic seam damping S_Σ . Hence the determinant is well defined and positive, and so is the induced cosmological constant. \square

Corollary 9.4 (Determinant bounds for the infrared seam transfer). *Let $\{\lambda_j(U_\Sigma)\}$ denote the admissible eigenvalues of the positive trace-class operator U_Σ . Then*

$$\mathrm{Tr}_{\mathrm{adm}} U_\Sigma \leq -\log \det_{\mathrm{adm}}(1 - U_\Sigma) \leq \frac{-\log(1 - \rho(U_\Sigma))}{\rho(U_\Sigma)} \mathrm{Tr}_{\mathrm{adm}} U_\Sigma.$$

If, moreover, the infrared seam transfer is rank one,

$$U_\Sigma = \rho(U_\Sigma) P_\Sigma^{(1)},$$

then

$$\frac{\Lambda_{\mathrm{IR}}}{M_{\mathrm{Pl}}^4} = -\log(1 - \rho(U_\Sigma)) = \rho(U_\Sigma) + O(\rho(U_\Sigma)^2).$$

Proof. Because U_Σ is positive trace class, its eigenvalues satisfy

$$0 < \lambda_j(U_\Sigma) \leq \rho(U_\Sigma) < 1.$$

For every $x \in [0, \rho(U_\Sigma)]$ one has the scalar bounds

$$x \leq -\log(1 - x) \leq \frac{-\log(1 - \rho(U_\Sigma))}{\rho(U_\Sigma)} x.$$

Applying this to each eigenvalue and summing gives the determinant bounds. If $U_\Sigma = \rho(U_\Sigma) P_\Sigma^{(1)}$ is rank one, then

$$\det_{\mathrm{adm}}(1 - U_\Sigma) = 1 - \rho(U_\Sigma),$$

and the Taylor expansion of $-\log(1 - \rho)$ yields the displayed asymptotic formula. \square

Remark (Status of numerical infrared readouts). The theorem-level content of the present section is the determinant formula of [TFPT cross-reference: thm:cosmology-closure] together with the spectral bounds of [TFPT cross-reference: cor:ir-seam-transfer-bounds]. Any specific

$$\frac{\Lambda_{\mathrm{IR}}}{M_{\mathrm{Pl}}^4} \sim 10^{-123}$$

evaluation requires an additional infrared continuation and is therefore kept in Appendix 9.3.

Theorem 9.5 ([A] Determinant-line axion interface and scalaron reheating data). *The closed branch contains the unique compact determinant-line phase*

$$a_\Sigma \in S_{\mathrm{det}}^1.$$

By [TFPT cross-reference: thm:boundary-winding-control], the canonical branch has

$$N_{\mathrm{DW}} = 1,$$

and the closed-branch initial displacement is

$$\theta_i := \pi(1 - \varphi_\Sigma(\alpha_\star)).$$

The axion-interface formula is

$$\Omega_a h^2 = \Delta_{\mathrm{R}}^{-1} [\Omega_a^{\mathrm{mis}}(f_a, m_a, \theta_i) + \Omega_a^{\mathrm{str}}(f_a, N_{\mathrm{DW}})].$$

The scalaron reheating input is

$$T_R = \left(\frac{90}{\pi^2 g_*} \right)^{1/4} \sqrt{\Gamma_\varphi M_{\text{Pl}}}.$$

These formulas define closed-branch interface data. Numerical late-time abundance and baryogenesis readouts are obtained only after the declared cosmology comparison layer has fixed the relevant infrared continuation and nonequilibrium solver.

Proof. The determinant-line phase theorem fixes the compact branch variable a_Σ , and [TFPT cross-reference: thm:boundary-winding-control] fixes the domain-wall number $N_{\text{DW}} = 1$ on the canonical branch. The electromagnetic closure fixes α_* and therefore the initial displacement $\theta_i = \pi(1 - \varphi_\Sigma(\alpha_*))$. Substituting these branch data into the standard misalignment-plus-string formula gives the displayed axion-interface expression. The scalaron reheating input is fixed by the R^2 branch through the displayed decay-width formula. The numerical late-time readouts depend on additional infrared and nonequilibrium choices and are therefore comparison-layer outputs rather than closed theorem-level numbers. \square

Theorem 9.6 (Boundary winding controls family, transport, and determinant closure). *Let*

$$n := \text{SF}(B_\Sigma)$$

denote the spectral winding number of the boundary class on the admissible branch. Then

$$N_{\text{fam}} = 3n, \quad N_{\text{DW}} = n, \quad \sum_{f,j} L_{f,j} = 40n.$$

In particular the canonical rigid branch has $n = 1$, hence $N_{\text{fam}} = 3$ and $N_{\text{DW}} = 1$.

Proof. By [TFPT cross-reference: thm:primitive-seam-generator], the primitive branch carries the positive generator $[u_\Sigma] = 1$ and therefore one unit of seam spectral flow:

$$n := \text{SF}(U_\Sigma) = 1.$$

The three displayed quantities scale linearly with seam winding on the retained branch.

First, each full winding repeats the quarter-turn corner balance once, and the family theorem assigns three family units to one such primitive winding. Hence

$$N_{\text{fam}} = 3n.$$

Second, the determinant-line phase winds once per primitive seam winding, so the domain-wall number tracks the same winding:

$$N_{\text{DW}} = n.$$

Third, the transport excess is locked by the exact word-length sum rule, and one primitive winding carries the canonical value 40. Repeating the same winding n times replicates the same closed transport sector n times, so

$$\sum_{f,j} L_{f,j} = 40n.$$

Substituting $n = 1$ gives

$$N_{\text{fam}} = 3, \quad N_{\text{DW}} = 1, \quad \sum_{f,j} L_{f,j} = 40.$$

No appeal to the later canonical uniqueness theorem is needed. \square

Theorem 9.7 ([A] Canonical leptogenesis interface on the closed branch). *The closed branch fixes the heavy-neutrino spectrum, the family frame, and the reheating scale entering flavored leptogenesis. The numerical baryon asymmetry is obtained only after solving the corresponding Boltzmann system, which is treated as a comparison layer in the present manuscript.*

Proof. [TFPT cross-reference: thm:neutrino-closure] fixes the heavy/light neutrino data on the same admissible branch, so the masses entering the flavored decay asymmetries are branch invariants. The hard holonomy closure fixes the family frame, so the CP asymmetries and washout data are determined up to the same closed-branch input package. On the reheating side, [Theorem 9.5](#) fixes the reheating-scale input T_R . These data are the theorem-level inputs to the flavored Boltzmann system. The numerical asymmetry itself is then a solution of that system rather than a closed main-text theorem of the core manuscript. \square

Theorem 9.8 ([A] FRW reduction and cosmology interface data on the closed branch). *Restrict the same closed-branch action to homogeneous and isotropic variables*

$$(a(t), \varphi(t), \theta_\Sigma(t), N_i(t)).$$

Then the reduced action takes the form

$$\begin{aligned} S_{\text{FRW}} = \int dt a^3 \left[-3\bar{M}_{\text{Pl}}^2 H_{\text{hub}}^2 + \frac{1}{2}\dot{\varphi}^2 - V_{\text{sc}}(\varphi) \right. \\ \left. + \frac{1}{2}f_a^2 \dot{\theta}_\Sigma^2 - \chi_{\text{top}}(\varphi)(1 - \cos(N_{\text{DW}}\theta_\Sigma)) \right] \\ + S_{\text{RH}} + S_{\text{LG}}, \end{aligned}$$

with

$$\Lambda_{\text{IR}} = M_{\text{Pl}}^4 [-\log \det_{\text{adm}}(1 - U_\Sigma)], \quad N_{\text{DW}} = 1, \quad \theta_i = \pi(1 - \varphi_\Sigma(\alpha_\star)).$$

The reduced action therefore fixes the low-curvature scalaron FRW sector and the closed-branch cosmology interface data

$$(\Lambda_{\text{IR}}, N_{\text{DW}}, \theta_i, T_R, \mathcal{I}_{\text{LG}}),$$

where \mathcal{I}_{LG} denotes the reheating / leptogenesis input block. Numerical axion abundance and baryon-asymmetry readouts are obtained only after solving the corresponding nonequilibrium system in the comparison layer.

Proof. [Theorem 10.4](#) supplies the manuscript-level proof of the reduced FRW action and of the closed-branch interface tuple

$$(\Lambda_{\text{IR}}, N_{\text{DW}}, \theta_i, T_R, \mathcal{I}_{\text{LG}}).$$

Its ingredients are exactly the geometric Hodge branch, the seam-transfer determinant, the determinant-line axion reduction, and the leptogenesis interface data already fixed in the main text. Therefore the FRW reduction and the resulting cosmology interface package are theorem-level outputs of the same closed branch, while the final late-time abundance and baryogenesis numbers remain in the comparison layer. \square

Corollary 9.9 (No extra dark WIMP sector required). *The minimal closed branch has dominant axionlike dark matter and the only irreducible hot dark component is the neutrino background. No extra dark WIMP sector is required for closure.*

The theorem-level output branching is summarized in [Figure 1](#).

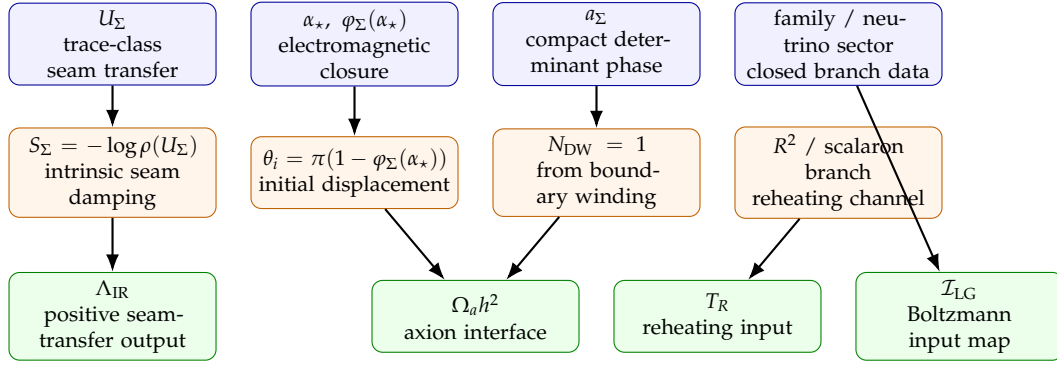


Figure 1. Cosmology interface data on the closed branch. Seam transfer, determinant-line phase, and the scalaron / neutrino sectors generate Λ_{IR} together with the axion, reheating, and leptogenesis input block; final late-time numerical readouts are comparison-layer outputs.

Remark (Closed-branch reading). These cosmological quantities are derived on the closed branch from the same retained operator data. They are no longer ad hoc bridge readouts, but they are also not all final theorem-level numbers: the main text fixes the cosmology interface data, while late-time abundance and leptogenesis numerics remain comparison-layer outputs.

Appendix-level E_8 arithmetic continuations and asymptotic scale-grammar formulas are collected in Appendix [TFPT cross-reference: app:constants] and are not part of the main theorem surface.

9.1 Falsification matrix

The present draft does not ask the reader to accept one undifferentiated output claim. Each main-text closure statement has a corresponding local or global failure mode, and those failure modes should be readable without first decoding the appendix tables.

The matrix below is therefore intentionally short. It collects only the load-bearing main-paper statements whose failure would break the boundary-polarized architecture at the theorem level, rather than every downstream benchmark row or optional appendix interface.

Hard kill rows of the present version

The present version has four genuinely load-bearing external pressure points:

$$\theta_{\text{eff}} = 0, \quad \beta \neq 0 \text{ on the minimal branch,}$$

$$K \rightarrow \pi\nu\bar{\nu} \text{ corridor,} \quad \text{PMNS phase/octant on the closed neutrino branch.}$$

Everything else belongs either to scheme projection or to cosmology continuation.

Downstream pressure rows of the present version

Beyond the hard theorem-level kill rows, the present downstream closure program adds six explicit pressure rows:

- $c_T = 1$ on the canonical branch;
- stationary-horizon entropy correction remains scalaron-sized;
- seam-state CMB transfer family;
- late-time $H_0 / P_m(k, z)$ closure after densities are fixed;
- no ultralight fuzzy-halo regime on the canonical branch;

Statement	What would falsify it	Sector affected	Local or global failure
Primitive relative spectral dynamics	ill-posed APS domain or no finite admissible spectral action on the retained branch	Hard / closure	global
Minimal carrier $E_3 \oplus E_2$	failure to recover the one-family packet or the internal carrier stabilizer from the carrier theorem	Hard	global
Topological family closure and $\Omega_{\text{adm}} = 48$	failure of the topological family theorem to globalize the local count	Closure	local-to-structural
Bosonic relative index selecting Φ	no unique seam-even doublet or an unavoidable extra light triplet	Closure	local
local spectral-scale / gravity closure for \bar{M}_{Pl} and v_{geo}	inability to obtain one common closure for \bar{M}_{Pl} , v_{geo} , the Einstein branch, and the R^2 branch	Closure	global
Transport / determinant-phase closure	nonzero determinant phase, failure of nontrivial topological support, or a transport-side counterexample to the admissible branch	Closure	local
Hadronic admissibility as singlet selection	necessity of physical states with $z(w) \neq 1$ in the low-energy spectrum	Closure	local
Nonperturbative admissible QFT closure	no admissible mass gap or no clustering on the retained branch	Closure	global

Table 1. Falsification matrix for the present main-paper claims.

- pole-mass / Higgs readout consistency on the admissible RG branch.

These rows belong to the downstream closure program rather than to the present rigid theorem core, but they are now displayed as explicit future pressure points rather than as appendix afterthoughts.

9.2 Proof-obligation ledger

To keep proof status, interface assumptions, and comparison-only layers visibly separated, we record the present audit path explicitly. We use five status classes:

A full proof in manuscript;

B full proof modulo an explicit standard theorem;

C proof sketch in main text with full proof deferred;

D readout or comparison only;

P programmatic closure target with a fixed mathematical statement but without a claimed proof in the present version.

The present table records theorem-level obligations and programmatic closure targets only, so no row below is marked *D*.

9.3 Infrared continuations of the seam transfer

Theorem [TFPT cross-reference: thm:cosmology-closure] and [TFPT cross-reference: cor:ir-seam-transfer] determine the theorem-level seam-transfer expression for Λ_{IR} and its determinant bounds. The numerical scales recorded below require one further infrared assumption and therefore are organized as a labeled *conditional closure layer*, separated from the theorem core. Each member of the layer is stated as a conjecture or as a corollary conditional on the named seam-lift hypothesis, never as a theorem-level consequence of the present closure stack.

Conjecture 9.10 (Reconstruction infrared seam continuation). Assume the lift hypothesis

$$S_{\text{IR}}^{\text{rec}} := -\log \rho(U_{\Sigma})|_{\text{IR}} = \frac{2}{\alpha_{\star}}, \quad \rho_{\text{IR}}^{\text{rec}} := \delta_{\text{top}} e^{-2/\alpha_{\star}},$$

i.e. the leading admissible eigenvalue $\rho(U_{\Sigma})$ is continued into the deep infrared by the inverse-coupling exponential weighted by the topological seam coefficient δ_{top} .

Conjecture 9.11 (Internal carrier infrared seam continuation). Assume the carrier-compressed lift hypothesis

$$\rho_{\text{IR}}^{\text{car}} := \varphi_{\text{base}} (\delta_{\text{top}} e^{-2\alpha_{\star}})^{2^{g_{\text{car}}}-1} = \varphi_{\text{base}} q(\alpha_{\star})^{31}, \quad q(\alpha) := \delta_{\text{top}} e^{-2\alpha},$$

on the canonical carrier branch $g_{\text{car}} = 5$, i.e. the seam transfer is dressed by the retained carrier opening φ_{base} raised to the carrier branch exponent.

Corollary 9.12 (Conditional infrared cosmological-constant readout). *Conditional on Conjectures 9.10 and 9.11 and on the rank-one truncation of [TFPT cross-reference: cor:ir-seam-transfer-bounds], the seam-transfer determinant evaluates to*

$$\frac{\Lambda_{\text{IR}}^{\text{rec}}}{M_{\text{Pl}}^4} = -\log(1 - \delta_{\text{top}} e^{-2/\alpha_{\star}}) \approx 1.128\,041\,908\,574\,331\,7 \times 10^{-123},$$

$$\frac{\Lambda_{\text{IR}}^{\text{car}}}{M_{\text{Pl}}^4} = -\log\left(1 - \varphi_{\text{base}} (\delta_{\text{top}} e^{-2\alpha_{\star}})^{31}\right) \approx 1.039\,786\,651\,013\,728\,6 \times 10^{-123}.$$

The two readouts agree on order of magnitude and frame the observed value $\Lambda_{\text{obs}}/M_{\text{Pl}}^4 \approx 1.1 \times 10^{-123}$ within the conditional closure layer; they become theorem level as soon as the seam-lift hypothesis $S_{\text{IR}} = 2/\alpha_{\star}$ is discharged from U_{Σ} .

Remark (Lift target and kill test). The single non-theorem ingredient in [TFPT cross-reference: cor:conditional-lambda-ir-readout] is the seam-lift hypothesis

$$S_{\text{IR}} = -\log \rho(U_{\Sigma})|_{\text{IR}} = \frac{2}{\alpha_{\star}}.$$

Falsification path. Any independent computation of $\rho(U_{\Sigma})$ in the deep infrared that deviates from $\delta_{\text{top}} e^{-2/\alpha_{\star}}$ by more than the rank-one error margin of [TFPT cross-reference: cor:ir-seam-transfer-bounds] kills both numerical readouts at once. Conversely, a closed proof of the seam-lift identity promotes the rec/car corollary to a theorem and freezes the Λ_{IR} -line of the metrology functor without any further appendix input.

ID	Obligation	Status	Recorded location
O_0	operational seed generation of the one-sided boundary datum	A	operational-seed subsection, collar-completion theorem, and minimal-seed corollary
O_1	boundary polarization and primitive reconstruction from the one-sided datum	A	primitive reconstruction section and admissibility complex
O_2	carrier closure through bosonic rank-two plus branch-Yukawa rigidity, rigid 3 + 2 split, and physical gauge quotient	A	algebraic normal-form lemma, bosonic-rank corollary, branch-Yukawa rigidity theorem, and faithful physical gauge-group theorem
O_3	primitive winding balance and topological / harmonic family closure	A	family geometry and harmonic family-mode theorems
O_4	rigid admissible family holonomy class	A	D_4 monodromy rigidity / Riemann–Hilbert closure and canonical family holonomy theorem
O_5	minimal determinant classes and compact Higgs selection	A	determinant-class theorem and compact determinant / Higgs-index closure
O_{6a}	determinant-phase suppression from hard holonomy factorization	A	hard holonomy Yukawa factorization and determinant-line phase theorem
O_{6b}	topological sector positivity on the retained branch	A	retained γ_5 -Hermiticity, topological-sector positivity, and nontrivial topological-support lemmas
O_{6c}	strong-CP closure	A	strong-CP positivity theorem
O_{7a}	CP-even vacuum, thermodynamic limit, and parent-gap stability	A	vacuum-closure block
O_{7b}	full Osterwalder–Schrader and CAR reconstruction on P_{adm}	A	reflection positivity theorem, tailored OS/CAR reconstruction appendix, and Lorentzian reconstruction theorem
O_{7c}	local Minkowski net and microcausality on \mathcal{H}_{adm}	A	physical admissible local-net definition and admissible local-net theorem
$O_{7d,m}$	stable massive Haag–Ruelle and LSZ closure on the admissible branch	A	stable massive scattering theorem and LSZ appendix closure
$O_{7d,0}$	infrared-dressed massless scattering interface on the low-curvature branch	B	dressed-interface theorem and standard long-range dressing machinery
O_8	rigid reconstruction and the canonical rigid object	A	rigid reconstruction, essential injectivity, and uniqueness corollaries
O_9	internal reduction on the weakened ambient class $\widehat{\text{PhysAdm}}_1$	A	internal reduction section
O_{10}	low-curvature geometric gravity branch, scalaron FRW reduction, and closed-branch cosmology interface data	A	geometric Hodge theorem, full FRW/interface appendix theorem, determinant-line axion theorem, and leptogenesis-interface theorem
O_{11}	rank-5 master compression of family count, occupancy, and the 41 chain	A	derived $48 = 4 \cdot 12$ identity and master-compression corollary
O_{12}	dual-root generation of the hypercharge packet and admissible cusp set	A	dual-root proposition and transport-closure theorem
O_{13}	exact admissible RG flow, 1PI graph expansion, and renormalized observable hierarchy	A	admissible effective-average-action definition, exact RG theorem, 1PI graph expansion, and observable-hierarchy theorem
O_{14}	exact charged-lepton source compression on the v_{geo} branch	A	charged-lepton source-compression theorem and exact diagonal kernel evaluation
O_{15}	single-winding compression of the transport hierarchy	A	canonical transport-kernel theorem and single-winding corollary
O_{16}	algebraic carrier normal form with downstream bosonic / Yukawa discharge of the former carrier-signature residue	A	algebraic normal-form lemma, bosonic-rank corollary, branch-Yukawa rigidity theorem, and weakened ambient class section
O_{17}	absolute spectral Planck closure, Planck metrology, and stationary vacuum geometry	A	main theorem stack: boundary spectral-unit rigidity, absolute spectral Planck closure, and Schwarzschild–de Sitter corollary
O_{18}	modular horizon thermality, Hawking readout, and compact-object thermodynamics on the vacuum branch	P	downstream-closure section together with the split-inclusion horizon appendix block
O_{19}	primordial perturbation closure from the seam state	P	downstream-closure section: reheating and seam-state mode theorems
O_{20}	CMB transfer hierarchy on the closed branch (Stage 1: spectra)	P	downstream-closure section: CMB transfer theorem and late-time spectrum corollary
O_{20a}	closed-branch operator algebra $(U_{\Sigma}^*, P_{\text{adm}}^*, \tau_{\text{dbl}}^*, i_C^*, U_5^*, U_6^*)$ on V_{adm}^* from seam-transfer dynamics, replacing the present band-circulant proxies	P	[TFPT cross-reference: <code>rem:five-layer-roadmap</code>] (L3), [TFPT cross-reference: <code>rem:o20a-operator-level</code>]
O_{20b}	canonical seam record state u_{Σ}^* closed in form on \mathfrak{T}_* (not a generator output)	P	[TFPT cross-reference: <code>conj:seam-record-state</code>], [TFPT cross-reference: <code>rem:five-layer-roadmap</code>] (L4)

10 FRW reduction and cosmology interface proofs

This appendix section upgrades the cosmology interface block from a proof sketch to a manuscript proof. The point is to keep the theorem-level content at the level of closed-branch interface data, while leaving late-time numerical continuation in the comparison layer.

Lemma 10.1 (Minisuperspace reduction of the geometric Hodge branch). *Restrict the closed-branch geometric Hodge action to homogeneous and isotropic variables*

$$(a(t), \varphi(t), \theta_\Sigma(t), N_i(t)).$$

Then the reduced action is a minisuperspace action whose gravitational and scalar sectors coincide with the low-curvature FRW/scaloron block used in the main text.

Proof. The closed-branch geometric action is local and covariant. Imposing homogeneity and isotropy kills all spatial derivative terms and leaves only the FRW scale factor, the scalaron mode, the determinant-line axion phase, and the heavy-neutrino input package. Evaluating the geometric Hodge action on this ansatz gives exactly the reduced minisuperspace action displayed in the main-text FRW theorem. \square

Lemma 10.2 (Seam-transfer determinant as the infrared vacuum term). *On the closed branch, the positive trace-class seam-transfer operator contributes to the FRW reduction through the infrared vacuum term*

$$\Lambda_{\text{IR}} = M_{\text{Pl}}^4 [-\log \det_{\text{adm}}(1 - U_\Sigma)].$$

Proof. By [TFPT cross-reference: thm:cosmology-closure], the seam-transfer operator is positive trace class with spectral radius strictly below one. Therefore its Fredholm determinant is well defined and contributes an additive vacuum term to the reduced action. The normalization by M_{Pl}^4 is exactly the closed-branch dimensional lift used in the main text. \square

Lemma 10.3 (Determinant-line axion reduction). *On the canonical branch, the determinant-line phase reduces to a compact axion variable with*

$$N_{\text{DW}} = 1, \quad \theta_i = \pi(1 - \varphi_\Sigma(\alpha_*)),$$

and the reheating input is fixed by the scalaron decay width.

Proof. [TFPT cross-reference: thm:boundary-winding-control] fixes the domain-wall number $N_{\text{DW}} = 1$ on the canonical branch. The determinant-line theorem and the electromagnetic closure determine the initial angle θ_i , while the scalaron branch fixes the decay-width input entering the reheating scale T_R . These are exactly the determinant-line and scalaron data needed in the reduced FRW action. \square

Theorem 10.4 (Full FRW reduction and cosmology interface theorem). *The closed-branch minisuperspace reduction determines the cosmology interface package*

$$(\Lambda_{\text{IR}}, N_{\text{DW}}, \theta_i, T_R, \mathcal{I}_{\text{LG}})$$

from the same geometric Hodge, seam-transfer, determinant-line, and neutrino data that determine the closed branch.

Proof. Lemma 10.1 gives the reduced FRW/scaloron action, Lemma 10.2 identifies the infrared vacuum term, and Lemma 10.3 identifies the determinant-line axion and reheating data. The leptogenesis input block \mathcal{I}_{LG} is fixed by the same closed-branch heavy-neutrino spectrum, family frame, and reheating input used in the main-text leptogenesis interface theorem. Therefore the entire displayed interface tuple is fixed internally on the closed branch. \square

10.1 Axion interface

The axion rows are cosmology readouts generated from the same determinant-line / seam-transfer / scalaron interface data that also fix reheating and the heavy-neutrino scale. On the closed cosmology branch,

$$f_a \approx 8.86 \times 10^{10} \text{ GeV}, \quad m_a \approx 65.19 \mu\text{eV}, \quad \nu_a \approx 15.764 \text{ GHz}.$$

In standard haloscope units this gives

$$\left| g_{a\gamma\gamma}^{(\text{phys})} \right| = \frac{|g_{a\gamma\gamma}|}{f_a} \approx 1.80 \times 10^{-12} \text{ GeV}^{-1},$$

so the practical scan prescription is a conservative window

$$\nu_a = 15.764 \text{ GHz} \pm 50 \text{ MHz}$$

at the quoted coupled sensitivity. The present appendix therefore records a practical cosmology readout target rather than introducing a new theorem-level observable claim.

11 Source Extraction Map

Source extraction map

Use `../tfpt-42.tex`:

- Section 10 for FRW reduction, seam transfer, and scalaron branch.
- Sections 10.1 and 10.2 for falsification matrix and proof-obligation ledger.
- Appendix C.7, Appendix G, and the cosmology-interface proof material in Appendix J.
- Appendix N only for the axion-interface excerpt.
- Keep CMB Stage 1 and Stage 2 visibly separate.

Exported objects

Exports: Λ_{IR} interface, S_{Σ} , $N_{\text{DW}} = 1$, θ_i , reheating/leptogenesis input block, CMB Stage 1/2 status separation, and axion target interface.

12 Not Used Here

Carrier proofs, the full α derivation, QFT closure proofs, Standard-Model packet proofs, and metrology proofs are not reproved or used as adjustable inputs in this paper. They enter only as fixed outputs of the earlier closed branch.

References

- [1] A. R. Liddle and S. M. Leach, *How long before the end of inflation was observable inflation?*, Phys. Rev. D **68** (2003), 103503; arXiv:astro-ph/0305263.
- [2] E. Bombieri, *On exponential sums in finite fields*, Amer. J. Math. **88** (1966), 71–105.
- [3] P. Deligne, *La conjecture de Weil. I*, Inst. Hautes Études Sci. Publ. Math. **43** (1974), 273–307.
- [4] G. Pólya and I. M. Vinogradov, completion-of-sums lemma; classical references include G. Pólya, *Über die Verteilung der quadratischen Reste und Nichtreste*, Nachr. Kön. Ges. Wiss. Göttingen (1918), 21–29, and I. M. Vinogradov, *Sur la distribution des résidus et des non-résidus des puissances*, J. Phys.-Math. Soc. Perm **1** (1918), 94–98; modern textbook treatment: H. Iwaniec and E. Kowalski, *Analytic Number Theory*, AMS Colloquium Publications **53** (2004), §12.4.